Effect of air pockets on pipeline surge pressure

R. Burrows, BEng, PhD, CEng, MICE, MCIWEM, and D. Q. Qiu, BEng, MPhil

Proc. Instn Civ. Engrs Wat., Marit. & Energy, 1995, **112**, Dec., 349–361

Water Board Water Panel Paper 10859

Written discussion closes 15 February 1996

■ **Through a series of analytical examples, it is demonstrated how the presence of air pockets can severely exacerbate surge peaks during pump shut-down in single water pipeline systems when operating unprotected against transient pressures. Single air pockets of small size and the multiple presence of air pockets are shown to be especially problematic. It is suggested that such behaviour may trigger pipe failures in circumstances where normal surge analysis may not predict such collapse.**

Introduction

Air pockets can develop in a pipeline by bubble entrainment through the action of pump suction and by air release from solution as the water pressure reduces. The former can arise from poor suction (wet) well design and through operation cycling which permits excessive drawdown before pump switching or shut-down. The amount of air release from solution depends on the pressure reduction and other factors, but water at standard conditions may contain about 2% dissolved air by volume (Fox, 1977,[1] and Twort *et al.* 1994[2]). It is obvious that entrapped air will collect at high points along the pipe profile in the form of pockets and there is also always a likelihood of air collecting at a change of gradient in the pipeline, as shown in Fig. 1 (after Twort *et al.*, 1994[2]). It is common practice in water supply systems to provide automatic venting to prevent excessive accumulation and consequential flow constriction. In sewerage, however, the maintenance problem has led to frequent omission of air valves in favour of the provision of 'sluicing' facility only.

2. The effect of entrapped air on surge pressures experienced by a pipeline can be either beneficial or detrimental from an operational performance perspective, depending on the amount, the two phase regime of the mixture (whether homogeneous or slug) and the nature and cause of the transient. It is generally held that when free (undissolved) air, or gas, is present in a hydraulic system, it can greatly reduce the surge pressure levels because free air in a homogeneous mixture greatly increases the elasticity of the fluid, so reducing the pressure wave speed and enhancing surge damping (Wylie and Streeter, 1978,[3] Ewing, 1980[4]).

3. It has recently been demonstrated by Lee (1993),[5] however, that spatial and time variation in the degree of entrainment, and hence wave speed, during the transient process itself can amplify the positive peak pressure. These results were obtained from a numerical, 'variable wave speed', model which simulates instantaneous gas release or absorption as pressures change. Lee cites, in support of his findings, the experimental observations of higher first pressure peaks (than those predicted by normal, constant wave speed, water hammer theory) during pump shut-down reported by Whiteman and Pearsall (1959, 1962),[6,7] Dawson and Fox (1983)[8] and Jönsson (1985).[9] He emphasizes, however, that aspects of the physical modelling are unresolved and Thorley (1991)[10] suggests that the re-absorption process may be so slow that it can be ignored. Dawson and Fox attributed the observed increase in peak pressure to the cumulative effect of minor flow changes during the transient, while Jönsson proposed compression of an isolated air cushion adjacent to the check (reflux) valve after closure. This was justified by application of a numerical model using constant wave speed and elastic theory. He concluded that: 'one could only expect that the smaller the air volume is the larger the pressure peaks. On the other hand there is certainly a lower limit on the amount of air that could be described as behaving as a cushion'. It would appear that both the air release model and the vaporous cavity model are capable of simulating observed pressure amplification. Both Lee and Jönsson express the need for further research. Reality probably involves a combination of both processes, neither of which can be satisfactorily verified without the more comprehensive field data.

4. Martin (1976),[11] Wylie and Streeter (1978)[3] and Safwat *et al.* (1986)[12] also refer to the occurrence of serious pressure levels if the air is trapped either between two liquid columns (i.e. air occupies the entire pipe cross-section) or near a closed valve during the rapid acceleration of the adjacent column of liquid. Larsen and Burrows (1992)[13] report attempts to verify a numerical model against experimental observations from several pipeline systems during pump shut-down conditions and subject to risk of cavitation: only by the incorporation of air pockets at high points could satisfactory calibration to the recorded peak pressures be achieved.

5. Computerized 'waterhammer' analyses are completed routinely for pumped pipeline

R. Burrows, Reader, Department of Civil Engineering, University of Liverpool

D. Q. Qiu, Postgraduate Student, Department of Civil Engineering, University of Liverpool

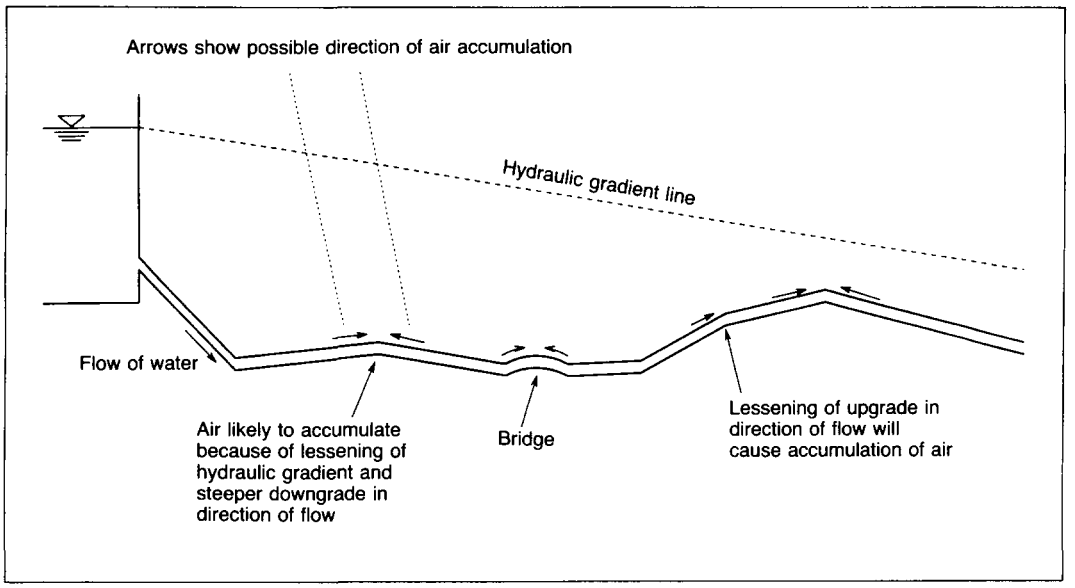

Fig. 1. Position of air accumulations

systems. The action of air valves, if present, can be readily incorporated. Where peak pressures are predicted to be excessive under foreseeable operational scenarios, surge suppression devices will normally be incorporated in the design. It is worthy of note that, in certain circumstances, air valves can exacerbate peak surge pressures—e.g. under pump shut-down—but this risk is easily identified as part of the computational study.

6. Air accumulations in the pipeline are both unintended and unquantifiable and, as a consequence, their potential influence on pressure transients is not given consideration, either at design stage or in post-failure inquiry. Situations where severe transients may arise include system malfunction, temporary operation during maintenance and repair, or even during normal pump trip-out. Jönsson (1994)[14] has shown that observation of pressure oscillations within a pipeline can be used to detect the probable location of gas pockets.

7. The objective of this article is to demonstrate the potential effect of entrapped free air, in pockets, on surge pressure levels during pump shut-down (including delayed pump trip-out) by way of several analytical examples based loosely on real single rising-main sewer systems.

Analytical approach

8. Entrapped air which collects at high points along the pipe profile or where the gradients change is not necessarily shifted by the water flow, especially on a downhill gradient where pockets at the soffit may not be able to travel backwards against the flow. Movement of the pocket in a forward direction may also be impeded in the case of a relatively flat main. Furthermore, any movement of air along a pipeline is slow. This movement can be ignored in comparison with the quick phenomenon of the travel of the 'waterhammer' pressure waves under transient analysis. Therefore, any air pockets can be assumed to remain in their original position during the time-scale of the hydraulic transients.

9. The analytical model used herein (Qiu, 1995)[15] for single pipeline systems was derived from the approach incorporated in the WHPS model developed by Larsen (1992),[16] employing standard procedures described fully by Wylie and Streeter (1978)[3] and Wylie (1984, 1985).[17,18] The principles can be summarized as follows.

(*a*) The standard method of characteristics is applied to convert the governing partial differential equations, describing 'waterhammer' phenomena in pipes, into ordinary differential equations. These are then solved along the lines of characteristics in finite-difference form with first-order approximation and without interpolation, so eliminating introduction of numerical damping.

(*b*) The fluid remains homogeneous and either free of entrained air/gas or at a constant air fraction content, such that pressure wave speed remains invariant during transient analysis.

(*c*) Air pockets of pre-selected sizes can be incorporated at chosen nodal points. It is assumed that the increment of air pocket volume does not cause water column separation during the transients, i.e. the gas in the air pocket does not occupy the entire cross-section of the pipe, as illustrated in Fig. 2.

(*d*) The gas in the air pocket is assumed to follow the reversible polytropic relationship detailed later. The absolute pressure head inside the air pocket is assumed to be equal to the gauge pressure at the nodal

points plus atmospheric pressure head (10·0 m water). Of necessity, no cavitation can occur at nodes where air pockets of finite size exist.

(*e*) The actual pipe diameter and cross-section area are used in the application of the method of characteristics at nodal points containing air pockets (see Fig. 2(b). No influence of the pocket on local pipe friction is considered, therefore, and no computation is made of its longitudinal extent. Output from the calculations does, however, include the maximum volumetric excursions of the air pocket during the analysis.

(*f*) Pipe friction is included in the model and pumping station losses (inlet, valves, bends, manifolds and expansions) are all characterized through a single head loss coefficient (ζ) applied to the kinetic head in the pipeline. Presence of check valve protection downstream of the pump is built into the modelling procedure, but additional bypass provision (with check valve) can be specified to protect a delivery line control valve against cavitation.

(*g*) Pump dynamics are specified through its lift/flow ($HP - Q$) characteristic, speed of rotation (N) and overall moment of inertia (I). In modelling pump run-down, a quadratic characteristic is assumed

$$HP = \beta_1 + \beta_2 Q + \beta_3 Q^2$$

and as the rotation speed changes, the pump characteristics satisfy the similarity relationships for homologous pumps, as described in Appendix 1.

10. For computational convenience, the position of air pockets is restricted to node points, representing junctions between adjacent pipe reaches, into which the pipe length is broken down. Neglecting velocity head, which is small, the total head above the datum at junction $[j, N(j) + 1]$ can be determined from the following compatibility equations for the fluid transients defined at the end of each computational time step Δt

$$C^+: \; H_{P[j,\,N(j)+1]} = C_{P[j,\,N(j)]} - B_j Q_{P[j,\,N(j)+1]} \quad (1)$$

$$C^-: \; H_{P(j+1,\,1)} = C_{m(j+1,\,2)} + B_{j+1} Q_{P(j+1,\,1)} \quad (2)$$

where

$$\begin{cases} C_{P[j,\,N(j)]} = H_{[j,\,N(j)]} + B_j Q_{[j,\,N(j)]} - \dfrac{f_j \Delta x_j}{2gD_j A_j^2} Q_{[j,\,N(j)]} \left| Q_{[j,\,N(j)]} \right| \\ C_{m(j+1,\,2)} = H_{(j+1,\,2)} - B_{j+1} Q_{(j+1,\,2)} + \dfrac{f_{j+1} \Delta x_{j+1}}{2gD_{j+1} A_{j+1}^2} Q_{(j+1,\,2)} \left| Q_{(j+1,\,2)} \right| \\ B_j = \dfrac{c_j}{gA_j} \qquad B_{j+1} = \dfrac{c_{j+1}}{gA_{j+1}} \end{cases}$$

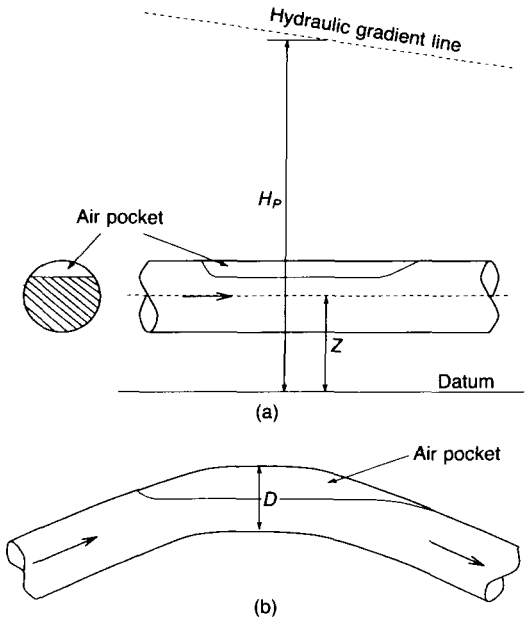

Fig. 2. Definition sketch

in which the subscript P indicates an unknown variable at the end of the time step under consideration, i.e. at time $t + \Delta t$, while a variable without the subscript P refers to its known value at the beginning of the time step, i.e. at time t; for the junction (j, i), the first subscript j ($j = 1, 2, \ldots, JJ$) refers to the pipe section between input topographical coordinates, and assumes a linear grade. The second subscript i ($i = 1, 2, \ldots, N(j) + 1$) denotes further subdivision into $N(j)$ reaches, of the jth pipe section; Q is the discharge; c is the wave celerity; Δx is the reach length; g is gravitational acceleration; f is the Darcy–Weisbach friction factor; D is pipe diameter and A is pipe cross-section area; B, C_P and C_m are constants of the compatibility equations. If the losses at the junction are neglected, then

$$H_{P[j,\,N(j)+1]} = H_{P(j+1,\,1)} = H_P \quad (3)$$

11. For stability of the numerical scheme, it is necessary to satisfy the Courant condition (Chaudhry, 1985[19]), i.e.

$$C_N = c\Delta t/\Delta x \leqslant 1{\cdot}0$$

Most accurate results are obtained with $C_N = 1$ (Wylie and Streeter, 1978[3] and Chaudhry, 1985[19]) and this condition ($\Delta x = c\Delta t$) has been taken here.

12. In a pipeline broken into several sections j, to accommodate changes in structure or perhaps topographical detail, a decision is needed in respect of the discretization of each section into $N(j)$ reaches of equal length Δx_j. Since Δt is fixed and the reach lengths Δx_j will differ at least marginally, slight adjustment of the 'target' wave speed is necessary if the equality limit is taken for the Courant condition. This approach has been taken herein, and an illustration of the effect can be seen in the

Table 1. Influence of time step selection for calculations of transients in pipeline profile 'b' of Fig. 3

Time step: s	$\Delta t = 0{\cdot}01$	$\Delta t = 0{\cdot}02$	$\Delta t = 0{\cdot}05$	$\Delta t = 0{\cdot}1$	$\Delta t = 0{\cdot}2$
Number of reaches	$N_1 = 124$ $N_2 = 82$ $N_3 = 102$ $N_4 = 178$	$N_1 = 62$ $N_2 = 41$ $N_3 = 51$ $N_4 = 89$	$N_1 = 24$ $N_2 = 16$ $N_3 = 20$ $N_4 = 35$	$N_1 = 12$ $N_2 = 8$ $N_3 = 10$ $N_4 = 17$	$N_1 = 6$ $N_2 = 4$ $N_3 = 5$ $N_4 = 8$
Adjusted wave speed: m/s	$c_1 = 301.6$ $c_2 = 302{\cdot}4$ $c_3 = 302{\cdot}0$ $c_4 = 320{\cdot}2$	$c_1 = 301{\cdot}6$ $c_2 = 302{\cdot}4$ $c_3 = 302{\cdot}0$ $c_4 = 320{\cdot}2$	$c_1 = 311{\cdot}7$ $c_2 = 310{\cdot}0$ $c_3 = 308{\cdot}0$ $c_4 = 325{\cdot}7$	$c_1 = 311{\cdot}7$ $c_2 = 310{\cdot}0$ $c_3 = 308{\cdot}0$ $c_4 = 335{\cdot}3$	$c_1 = 311{\cdot}7$ $c_2 = 310{\cdot}0$ $c_3 = 308{\cdot}0$ $c_4 = 356{\cdot}2$
CPU time UNIX: s	117·76	31·45	8·23	3·17	1·63
CPU time PC: s	592·39	169·18	39·60	17·03	9·77
At pump exit H_{max}/H_{min}	45·358 /13·071	45·355 /13·071	45·652 /13·067	45·471 /13·067	44·724 /13·011
At junction 1 H_{max}/H_{min}	43·6143 /12·895	43·610 /12·938	43·603 /13·062	43·759 /13·102	44·002 /13·220
At junction 2 H_{max}/H_{min}	40·237 /15·065	40·232 /15·065	40·665 /15·048	41·289 /15·062	42·392 /15·092
At junction 3 H_{max}/H_{min}	35·501 /16·362	35·497 /16·364	35·744 /16·403	35·851 /16·388	36·643 /16·206

Target wave speed: $c_1 = 300{\cdot}0$; $c_2 = 300{\cdot}0$; $c_3 = 300{\cdot}0$; $c_4 = 320{\cdot}0$
Steady-state air pocket volume = 0·05 m^3

figures in Table 1. The alternative is to retain fixed wave speed, thereby tolerating differential values of C_N (but <1) for each pipeline section.

13. In the analysis of the air pocket acting as a simple accumulator, shown schematically in Fig. 2(a), the pressure at any instant is assumed to be the same throughout the volume. The gas is assumed to follow the reversible polytropic relation

$$H_A V^n = Co \tag{4}$$

in which the absolute pressure head $H_A = H_P - Z + \bar{H}$, where $\bar{H}$ is barometric pressure head; Z is the elevation of pipe axis above the datum; V is the gas volume in the pocket; the polytropic exponent n varies in the range $1 \sim 1{\cdot}4$, an average value of $n = 1{\cdot}2$ generally being taken in calculations (Wylie and Streeter, 1978[3]); Co is a constant determined from the initial steady-state condition for the air pocket. Since equation (4) may apply at any instant, it is written for junction $[j, N(j) + 1]$ at the end of the time increment Δt, as

$$(H_P + \bar{H} - Z_{[j,\,N(j)+1]}) \times (V_{[j,\,N(j)+1]} + \Delta V_{[j,\,N(j)+1]})^n = Co \tag{5}$$

In this equation, V is the air volume at the beginning of the time step Δt; ΔV is the air volume change during the Δt time interval. The continuity equation for the junction becomes

$$\Delta V_{[j,\,N(j)+1]} = \frac{(Q_{P(j+1,\,1)} - Q_{P[j,\,N(j)+1]}) + (Q_{(j+1,\,1)} - Q_{[j,\,N(j)+1]})}{2}\,\Delta t \tag{6}$$

14. Substituting Equations (1) through (3) and (6) into equation (5) and eliminating $Q_{P[j,\,N(j)+1]}$ and $Q_{P(j+1,\,1)}$ and replacing $H_{P[j,\,N(j)+1]}$ and $H_{P(j+1,\,1)}$ by H_P yields

$$\left[V_{[j,\,N(j)+1]} + \frac{\Delta t(Q_{(j+1,\,1)} - Q_{[j,\,N(j)+1]})}{2} - \frac{\Delta t(B_j C_{m(j+1,\,2)} + B_{j+1} C_{P[j,\,N(j)]})}{2(B_j B_{j+1})} + \frac{\Delta t(B_j + B_{j+1})}{2(B_j B_{j+1})} H_P\right]^n (H_P + \bar{H} - Z_{[j,\,N(j)+1]}) = Co \tag{7}$$

H_P is the only unknown in equation (7), which is a non-linear equation and the Newton method is employed for solution.

15. Given that Co is a positive coefficient evaluated when an air pocket size is specified under steady flow conditions and that H_A is constrained to positive values, it is clear that

the computation scheme ensures that air volume is always evaluated as a positive quantity.

16. In addition to this treatment of air pockets, the numerical model considers also the potential for cavitation during the transient conditions. Vapour pockets will form as soon as the pressure in the pipe is reduced to vapour pressure (here taken as −10·0 m gauge). Upon occurrence of vapour pressure at an internal calculation point (node), the hydraulic grade line is then known at the section, and computation therefrom is treated as a boundary condition with known head. The computational modelling of column separation with constant wave speed is described fully by Wylie and Streeter (1978).[3]

17. The description of other boundary conditions imposed in the model are omitted herein, since they are treated in standard manner (Wylie and Streeter, 1978,[3] and Watters, 1979[20]).

18. The computational routine employed here, known under the name PTPSliv.FOR, was written in Fortran 77 coding and operated on Unix and PC platforms. It, together with its validation testing, is described fully in Qiu (1995).[15]

Application of the analysis to several pipeline configurations

19. The pipeline profiles investigated here are illustrated schematically in Fig. 3; all are of 6-bar rated PVC construction. Pipeline 'a' is a rising main with one high point and is taken from the demonstration example (No. 1) presented by Larsen (1992).[21] Pipeline 'b', with one high point, and pipeline 'c', with five distinct high points, are modelled loosely on sewer mains at Oue and Stovring, Denmark, as given in Larsen and Burrows (1992).[13]

20. Each system has single or multiple pumps, with one-way check valve, drawing from a sump at the upstream end and a reservoir boundary condition at the downstream end. The internal diameter of the pipeline and the salient elevations of the pipe axis above datum are summarized in Fig. 3.

21. Only pressure transients arising from pump shut-down are considered in this paper. In order to demonstrate the effect of the air pockets on surge pressures, protection devices were not considered in the systems for other than the first introductory example. The effect of an assumed pump inertia is, however, taken into account in all the applications.

22. Figure 4 shows the maximum and minimum head envelopes in pipeline 'a', sketched in Fig. 3(a). The envelope representing conditions with surge suppression (no air pockets, $V = 0{\cdot}00$) was obtained by introduction of an air chamber, with an initial 0·4 m^3 air volume, located immediately downstream of the pump check valve. This solution conforms to 'example 2' in Larsen (1992)[21] and provides a validation check on the computational routines. More importantly, however, it provides an illustration of an acceptable design where peak transient pressure never exceeds normal (steady state) dynamic values, and minimum pressures never fall close to −10·0 m (gauge), so eliminating cavitation risk. Time variation of surge pressure at pump exit, the first nodal point of the delivery pipe, is shown in Fig. 5.

23. Without the benefit of the surge suppression measure, results show ($V = 0{\cdot}00$) a general enhancement of peak pressures, and extended sections of the pipeline are subject to cavitation, the minimum head envelope being constrained at 10·0 m below pipe elevation in Fig. 4. With the approach to full vacuum pressure, the water 'boils' and vapour cavities form in the pipeline. the resulting 'water column separation' and subsequent cavity collapse, which occur both in practice and in the model, generate high local pressures and create spiky oscillations on the time traces, clearly evident in Fig. 5. Cavitation is, however, prevented at the pump exit by suction-drawn flow through the pump, and minimum head is, thereby, maintained at close to the sump elevation. This feature of the upstream boundary condition can create its own perturbation on the form of the transient wave cycles.

24. Limitations on the modelling of the cavitation phenomenon are that the wave speed is assumed to be unaffected by the cavitation process and that vapour cavity formation is constrained to the node points separating adjacent pipe reaches. Consequently, the numerical results are subject to greater levels of uncertainty in these circumstances, and Larsen (1992)[16] includes a small damping of the peaks in his WHPS model in accord with his experience. No such adjustment is made here, and the peak pressures simulated ($V = 0{\cdot}00$, in Fig. 4) are slightly higher than those shown in Larsen (1992).[21] It is worth emphasizing that cavitation is an unsatisfactory hydraulic condition by virtue of the high pressure peaks, risk of pipeline collapse or fatigue weakening, and good engineering design of the pipeline system will eliminate the problem by introduction of suitable suppression measures. Detection of the occurrence of cavitation is, therefore, the primary modelling goal in routine investigations rather than precise computation of ultimate peak pressure magnitudes.

25. The effect of the presence of an air pocket located at the high point ($x/L = 0{\cdot}53$; L is length of the pipeline and x is the distance from the pump at the upstream end) is also shown in Fig. 4. The initial steady-state air pocket volume selected in this case is 0·35 m^3, and volume variation during the transient is found to be between the maximum of 1·07 m^3

and minimum of 0·312 m^3. It can be seen that the air pocket has had a similar effect to the air chamber in this case, uplifting minimum pressures and suppressing maximum peak pressures. The resulting head fluctuations at pump exit, in Fig. 5, show considerable reduction but not complete elimination of the cavitation 'spikes' and the introduction of other oscillation cycles characteristic of both the partial reflection of the pressure waves from the air pocket and a longer period motion representing mass oscillation from the effect of the air void. The same air pocket volume located at $x/L = 0{\cdot}40$, representing an intermediate phase in its possible migration from the pump, was found to eliminate the cavitation. On the basis

Fig. 3. Pipeline profiles

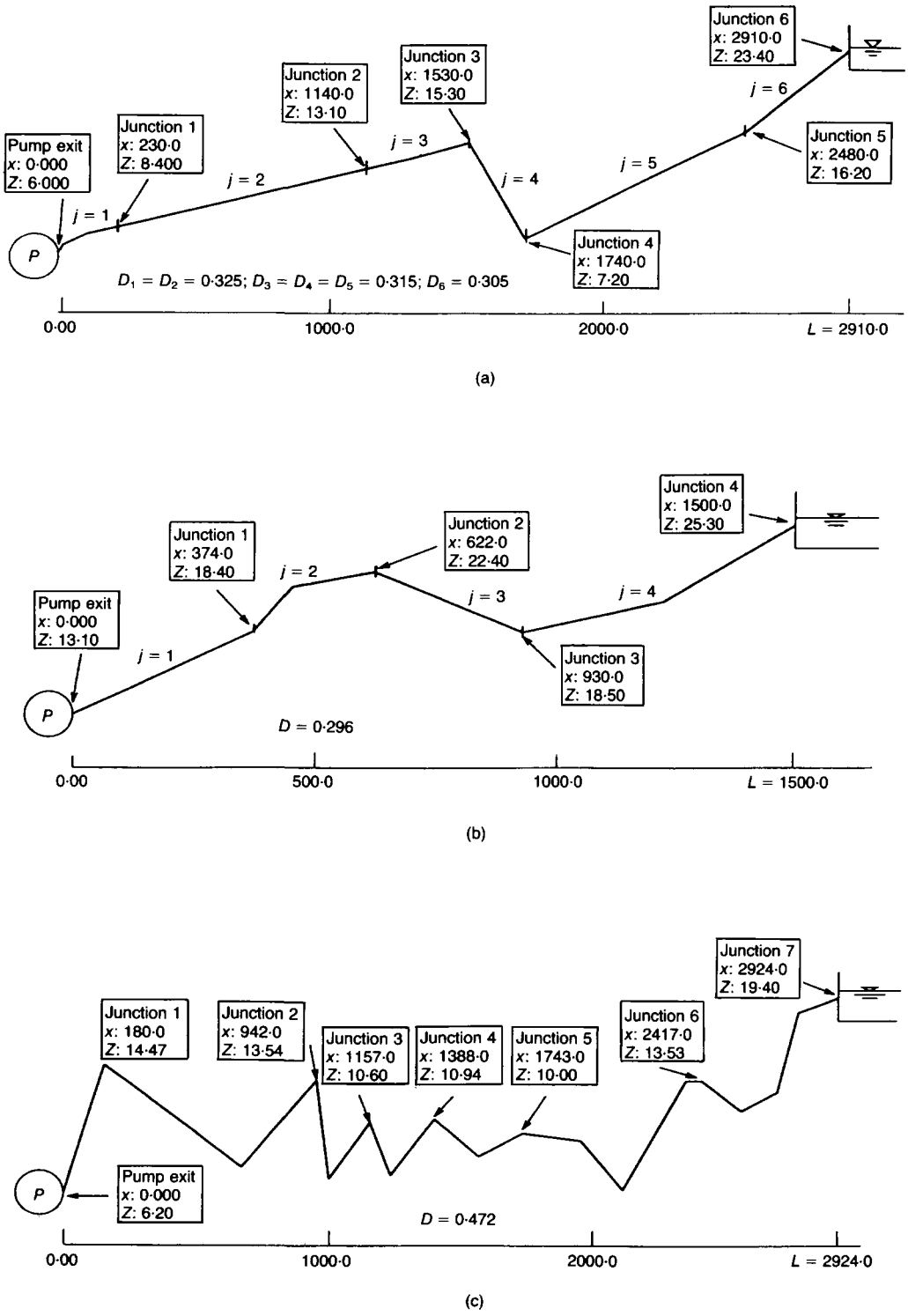

of the evidence presented in Figs 4 and 5, it appears that the working state of pipeline 'a' is considerably improved by the presence of this large air pocket.

26. Figures 6 and 7 show similar results for pipeline 'b' (Fig. 3), this time for various air pocket volumes at the high point ($x/L = 0{\cdot}41$). Flow conditions and important pipeline and pump characteristics are summarized in Fig. 6. It can be observed that, during the transient following pump shut-down, ultimate minimum head along the pipeline shows uplift as the air pocket volume is enlarged, except for the upstream section of the pipeline in the case of the smallest air pocket volume. Close inspection shows that with no air pocket ($V = 0{\cdot}000$), cavitation occurs along the approach to the high point, and rapid pressure fluctuations result on the time trace (Fig. 7). The influence of air presence on the ultimate maximum head is less consistent. For much of the pipeline profile, larger air pocket sizes are seen (in Fig. 6) generally to produce lower pressure peaks than when air is absent. The confused behaviour in the section of the pipeline upstream of the air pocket is caused by the superposition of the motion of pressure waves between the air pocket and the pump/check valve system and the mass oscillations introduced by the air void. The significance of these inconsistenceis in trend is, nevertheless, only marginal. More serious, however, is the substantial increase in peak pressures associated with a small air volume ($V = 0{\cdot}025$ m^3), the occurrence is seen clearly in the time series plotted in Fig. 7.

27. Stability checks on the computation procedure were made in response to these findings, and Table 1 presents some results. A range of time steps Δt, varying from 0·2 s (adopted as the standard for all investigations herein) to 0·01 s, were considered for application to pipeline 'b'. The smaller time steps were considered to introduce even greater accuracy into the finite difference calculations. Standard application of the Courant condition was made, and discretization of the pipeline, into equal length reaches within each section, forced slight adjustment to wave speeds. Good stability is shown over the entire range of times steps, in terms of both the head excursions listed in Table 1 and the time variations, a sample of which is shown in Fig. 8. The alternative discretization approach, discussed earlier, which fixes wave speed in each pipe section by varying the Courant number, was found (Qiu, 1995[15]) to have some influence on the predictions under cavitation, but this is not of significance to the comparative behaviour under investigation here.

28. The influence of air pocket volume is investigated systematically in Fig. 9, where ultimate maximum peak pressures are normalized in terms of the steady-state dynamic duty

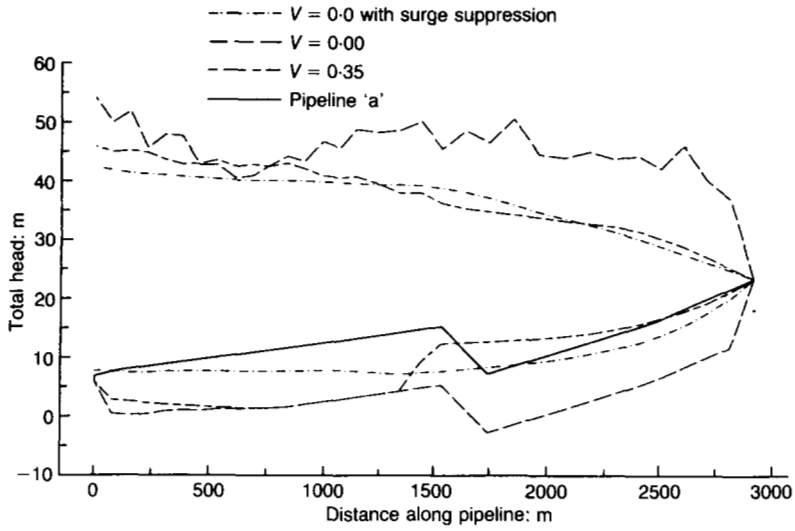

Fig. 4. Comparison of maximum and minimum head envelopes along pipeline 'a' (Fig. 3) following pump shut-down, with and without surge suppression and also with a single air pocket located at $x/L = 0{\cdot}53$ (Conditions: single pump with check valve, initial steady flow 98·9 l/s; pump inertia moment 0·3 kgm^2; pump characteristics ($\beta_1 = 60{\cdot}0$, $\beta_2 = -172{\cdot}3$, $\beta_3 = -537{\cdot}7$); pump speed N, 2900 rpm; sump level 6·02 m; surge suppression at pump delivery—air chamber start air volume 0·4 m^3; pipeline of pvc; station head loss coefficient ζ, 10·5)

pressures at the corresponding section. In the lower range, volume incrementation as small as 0·005 m^3 was considered in the computations. For this pipeline, a small air pocket volume of approximately 0·025 m^3 is seen to cause considerable enhancement of positive peak pressures at all four sections shown. Beyond a certain critical volume and downstream of the air pocket, the pressure head duty decreases with the increase of air pocket volume until optimum status is attained where initial steady-state (dynamic) pressures are not exceeded. For upstream sections of the pipeline, the picture is more confused; here, optimal air pocket volume

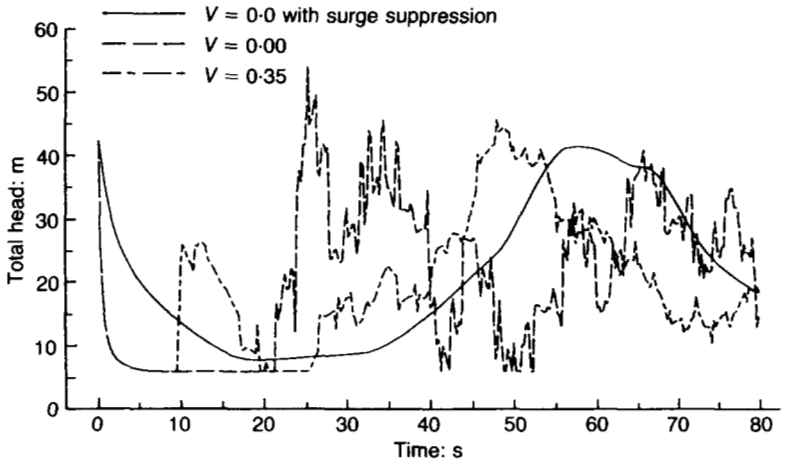

Fig. 5. Variation of surge pressure at pump exit in pipeline 'a' (Fig. 3), under conditions detailed in Fig. 4

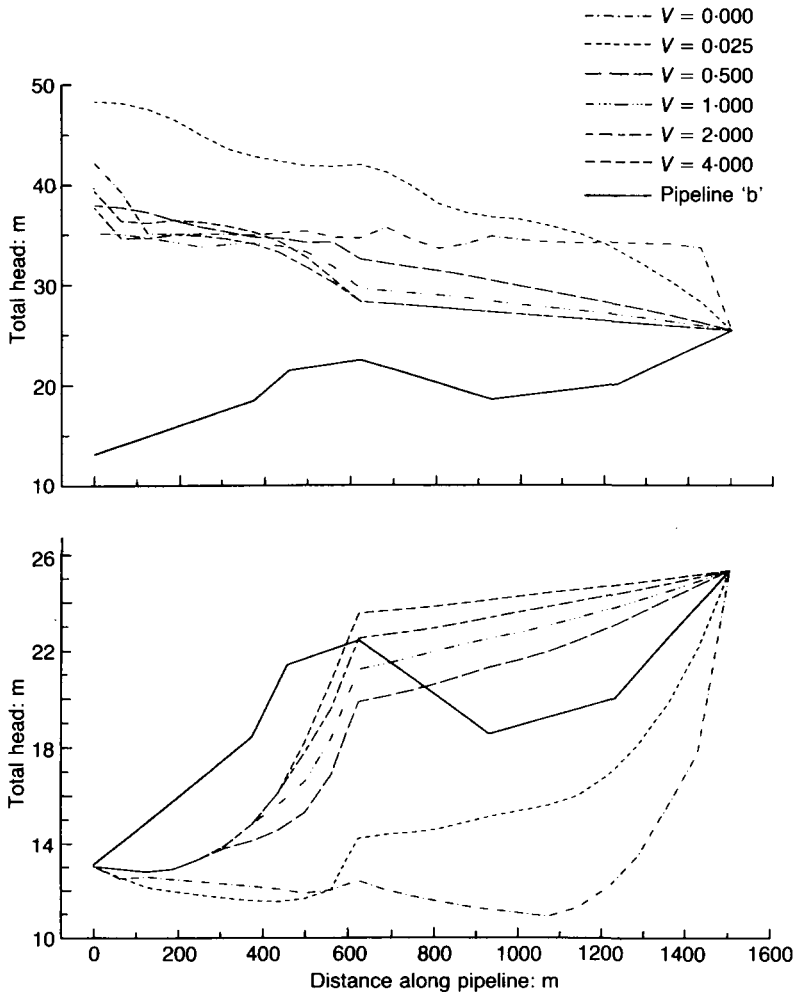

Fig. 6. Comparison of maximum and minimum head envelopes along pipeline 'b' with different air pocket volumes (located at $x/L = 0{\cdot}41$) (Conditions: single pump with check valve, initial steady flow 54·1 l/s; pump inertia moment 0·3 kgm^2; pump characteristics ($\beta_1 = 60{\cdot}0$, $\beta_2 = -516{\cdot}9$, $\beta_3 = -4838{\cdot}9$); pump speed N, 2900 rpm; sump level 13·11 m; pipeline of pvc; station head loss coefficient ζ, 10·5)

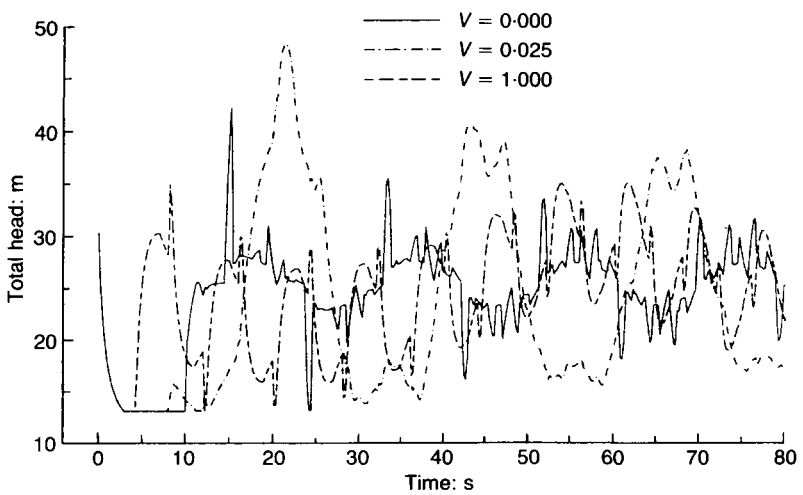

Fig. 7. Variation of surge pressure at pump exit with and without air pocket (at $x/L = 0{\cdot}41$) in pipeline 'b', under conditions detailed in Fig. 6

(that minimizing ultimate maximum pressure) is finite. If pocket size is increased further, some growth in transient pressures is caused, albeit to values closest to the figures produced when air is absent ($V = 0{\cdot}000$). The validity of the modelling becomes questionable for large air volumes since such accumulations would have frictional implications, and, in extreme cases, the computed volumes may extend across adjacent reach boundaries, whence modified computation should be made at the affected nodes. Neither of these aspects is currently incorporated.

29. On the basis of the evidence collected, the following hypothesis is offered for the effect of air voids. Following sudden change in operation, such as pump shut-down, pressure waves propagate back and forth along the pipeline, being reflected from the upstream and downstream boundaries while being damped by pipe friction. Intermediate air pockets introduce an energy source to the fluid flow system, and an internal boundary from which the pressure waves will be modulated and partially reflected. Moreover, by virtue of the cushioning effect of their volume change under pressure variations, they are able to bring about a more gradual deceleration of the flow by converting part of the rapid fluid transient into a more controlled mass oscillation. This action is comparable to that of an air chamber but without the additional friction damping provided by an outflow/inflow constriction. Small air pockets produce a mass oscillation period longer than the transient pressure wave frequencies, which are typically four times the travel time between relative boundaries. This period increases and the pressure amplitudes reduce as the air pocket size is enlarged.

30. Detailed scrutiny of Fig. 7, aided by other output data not included here, shows, for $V = 0{\cdot}025$ m^3, a mass oscillation of approximately 24 s period, with a first cycle amplitude of about 16 m head. Superimposed on this is a smaller oscillation characteristic of the transient oscillation between the pump/valve and the air pocket. Time series, at the sections considered in Fig. 9, confirm the time synchronization of the mass oscillations (Qiu, 1995[15]). The wave form arising from the behaviour of the air pocket is illustrated in Fig. 8, but here for the slightly larger volume of $V = 0{\cdot}05$ m^3. This form, with narrow peak and elongated trough, is characteristic of experimental observations of air accumulations (Jönsson, 1985[9]). For the larger air volume, $V = 1{\cdot}000$ m^3 a mass oscillation of much smaller amplitude, about 4 m head and 55 s period, arises. This pocket, however, now reflects a much stronger transient wave than the small air pocket such that the trace in Fig. 7 is dominated by this component. Downstream of the air pocket, stronger evidence of the transient pressure

waves is seen for the small air volumes, demonstrating less efficiency in the energy conversion to mass oscillation and the weaker reflective capability of the small pocket.

31. The findings in respect of the mass oscillation element of the behaviour are consistent with the conclusion of Jönsson (1985)[9] from his field observations and numerical analysis of air cushion formation in front of a pump check valve. In fact, Jönsson showed that the simpler inelastic, rigid column, analysis of the oscillating water between the upstream reservoir and the air pocket gave reasonable predictions. For small air volumes, with more rapid oscillations, Jönsson demonstrated the need for the elastic properties of the water column to be included by application of the waterhammer analysis, as considered here. With the air pocket at the check valve, the whole pipeline is subjected to the mass oscillation only, as demonstrated by Jönsson's results. When the air pocket is at an internal high point, the upstream section of the pipeline is still subject to the transient pressure cycles, as seen in Fig. 7, which now travel back and forth between the pump/check valve and the air pocket. In the case of large air pockets, the resulting pressure variations will be dominated by these transient fluctuations since the amplitude of mass oscillation will be small. This accords well with the field observations of delivery main pressures reported by Jönsson (1994)[14] and Larsen and Burrows (1992)[13]. This tendency for large air pockets to approach the action of a reservoir (constant head) boundary condition reduces the effective length of the pipeline and can so create larger transient peaks, as evident from the results in Fig. 9.

32. Figure 9 also investigates the influence of the polytropic exponent n, describing the behaviour of the gas in the pocket (see equation (4)). The exponent depends on the thermodynamic process followed by the gas in the pocket. If a perfect gas is assumed: at one extreme, the process may be isothermal, $n = 1{\cdot}0$; or at the other limit, it may be isentropic (reversible, adiabatic), $n = 1{\cdot}4$. For small chambers or accumulators with fast response times, the process may be taken as isentropic (Wylie and Streeter, 1978[3]). In larger systems with a larger water volume and small air mass, the transformation may approach an isothermal process. In order to examine the effect of polytropic exponents on surge pressure predictions, two extreme cases and one average case were considered in the foregoing analyses. it is clear from Fig. 9 that the value of the polytropic exponent is only of secondary importance in these studies. If not stated otherwise, a value of 1·2 has been assumed elsewhere herein.

33. The effect of air pockets on the pressure transients when the pipeline 'b' system is subject to delayed pump trip-out is shown in Figs 10 and 11. The second pump run-down is delayed by 25 s relative to that of the first pump. The air pocket is again located at the high point and the behaviour is similar to that for the sudden pump shut-down, there now being enhanced ultimate pressure duty along the entire pipeline when the air pocket size is very small (0·025 m^3). For the other air pocket volumes considered in Fig. 10, little change is seen in the maximum head envelopes. The delayed trip of the second pump assists surge suppression and maximum pressure experienced during a transient with no air present is the normal dynamic duty, represented by P(maximum)/P(steady state) = 1·0 in Fig. 11. This is seen also to be the case for air pockets of size greater than 0·5 m^3 at each section of the pipeline considered in Fig. 11.

34. The expanded scale of Fig. 11, against Fig. 9, makes clear the observation that different points along the pipeline will the susceptible to maximum peak pressure enhancement by air pockets of differing (small) size and also, although not illustrated here (Qiu, 1995[15]), to differing air pocket location.

35. For pipelines constructed over undu-

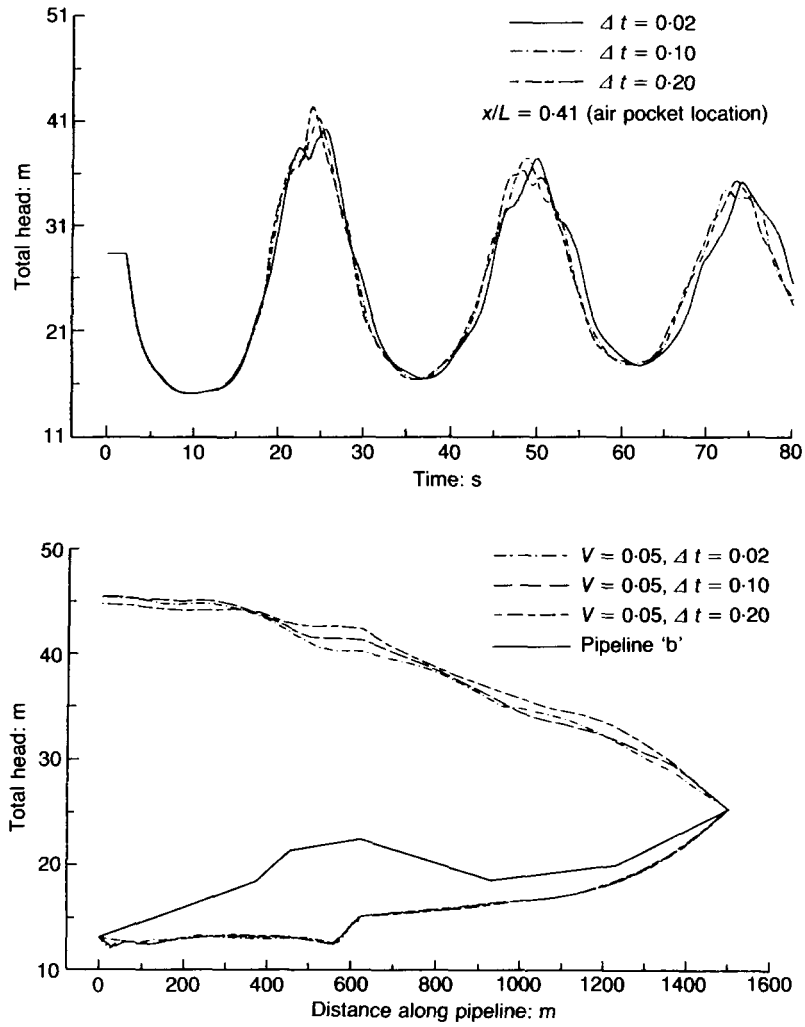

Fig. 8. Stability test on computational routines; maximum and minimum head envelopes and head profiles associated with results in Table 1

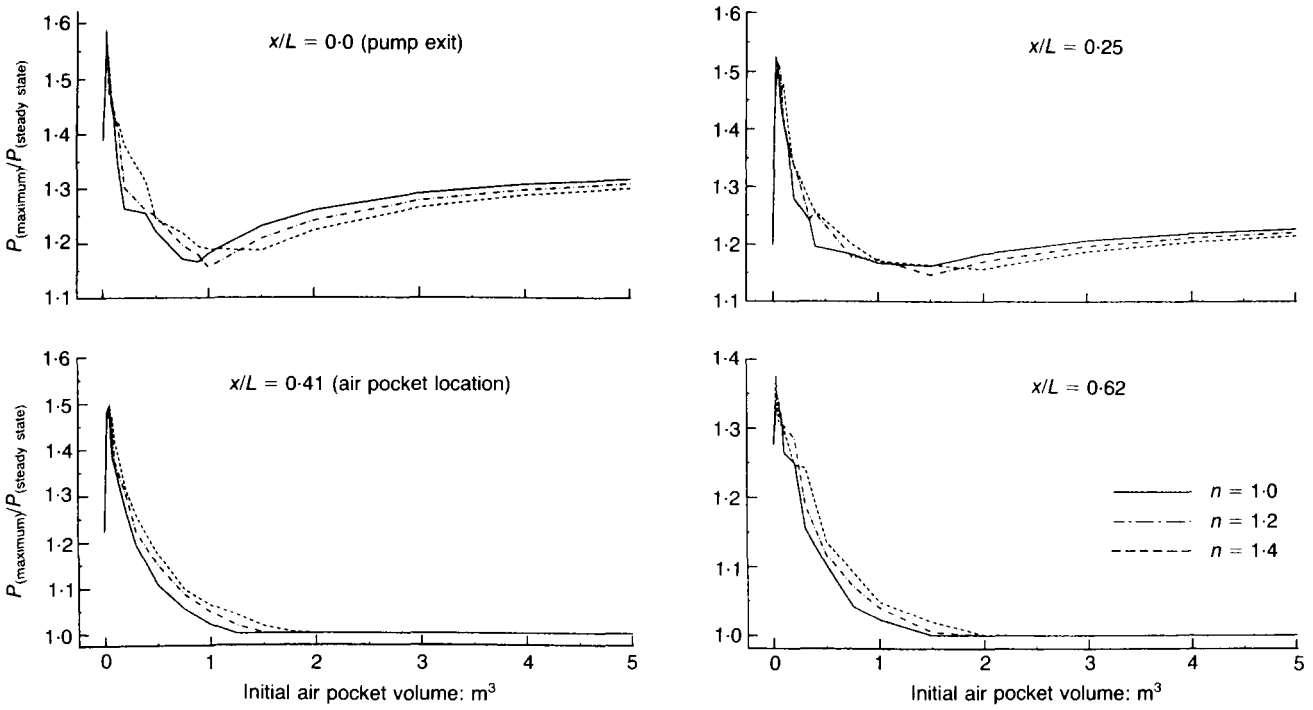

Fig. 9. Variation of ultimate maximum pressure duty, at sections along pipeline 'b', with increase in air pocket size (effect of polytropic exponents also illustrated)

lating terrain, it is possible that air pockets may form at each of a multiple set of high points along a pipeline. It is of interest, therefore, to investigate whether or not the increased degrees of freedom for transient wave motions and mass oscillations may exacerbate resulting pressures. Pipeline 'c' in Fig. 3 has been chosen for this study; details of the initial flow conditions, pump and pipeline characteristics, as well as results arising, are presented in Fig. 12. The steady-state total air pocket volume considered in these analyses, distributed over five high points along the pipeline, has been selected on the basis of: an equal distribution of pocket size; a linear increasing distribution of size working downstream; and a linear decreasing distribution. To facilitate a systematic study, the air volume distribution (to the different pockets) has been chosen arbitrarily using the relationship

$$V_k = V_0 + \gamma(k - 1) \tag{8}$$

where V_k is air volume at the kth high point; V_0 is the air volume at the first (upstream) high point; γ is a chosen constant (positive or negative).

36. Figure 12 shows the variation in the ratio between the maximum pressure experienced during the pump shut-down transient and the steady-state duty pressure, with change in air pocket volume at different locations (x/L) along the pipeline. It is observed that there is a considerable peak pressure enhancement, near or exceeding twice the steady-state dynamic head when total air volume is small (less than 0·5 m³ in this example). With increase in total air volume, the pressure enhancement generally reduces and peak pressure tends towards the steady-state value, except at pump exit. The most pertinent observation from these results is that for the entire range of air pocket volumes considered, the maximum transient pressures at the pump exceed those created when the pipeline possesses no air pockets. This pressure excess also arises at most locations along the pipeline even for significant air volumes (up to 3–4 m³). Stability of these solutions was again successfully tested by consideration of reduced time steps down ot 0·02 s (Qiu, 1995[15]).

37. When compared with the situation with only one high point in the pipeline, where peak pressure enhancement occurs only when air volume is very small, air in multiple pockets

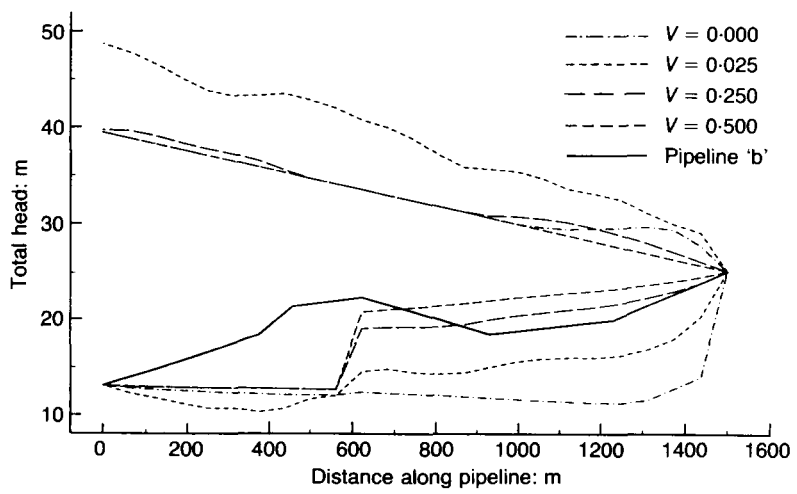

Fig. 10. Comparison of maximum and minimum head envelopes along pipeline 'b' with different air volumes (in pocket at $x/L = 0{\cdot}41$) subject to delayed pump trip-out (Conditions: as Fig. 6 except: two homogeneous pumps, total initial steady flow 90·81 l/s; second pump trip delayed by 25 s)

appears to cause a more general and greater risk to the pipeline system.

Conclusions

38. The examples presented in this paper have illustrated the varying influence that air pockets can have on the surge experienced in pipeline systems operated without the protection of surge suppression devices. In extreme cases, the high peak pressures arising might be expected to have a potentially catastrophic effect: peak pressure enhancements as high as 1·6 or even 2 times the normal steady-flow duty pressures have been predicted.

39. While a large air cavity acts as an effective accumulator and suppresses the maximum pressure excursions—following pump shutdown, for example—it seems that such volume split between multiple pockets can substantially exacerbate the peak pressures experienced. In either situation, the presence of only a small air volume (in these examples $<0{\cdot}5\ m^3$) is the cause of significant peak pressure enhancement.

40. The degree of peak pressure enhancement has been shown to depend on both the position of the air pocket in the pipeline and the location along the pipeline which is under scrutiny. The quantitative data presented herein are specific to the pipeline configurations investigated and no attempt at transposal to other situations is justified.

41. The potential impact of air entrainment in pipeline systems has been widely understood for some time by researchers in the field, and the topic is covered extensively in the literature, only a small sample from which has been cited here. Field evidence of peak pressure enhancements have been reported by Jönsson (1985)[9] and Larsen and Burrows (1992),[13] among others, and both offer mathematical treatment in the manner outlined here as the means for satisfactory synthesis of the pipeline transients. Lee (1993),[5] however, advocates the simulation of gas release and re-absorption, in a variable wave speed model, in order similarly to reproduce the observed high pressure peaks. A need clearly remains for further controlled high quality data, from field or laboratory experimentation, to enable absolute verification of the modelling approaches.

42. No new theoretical advance on the subject is offered in this paper; it has been the authors' aim simply to demonstrate, by systematic computer synthesis, the potentially adverse impact of air accumulation on pipeline systems unprotected against surge, and to bring it to the notice of the profession at large.

43. From first-hand experience of one post-failure inquiry, it proved impossible to demonstrate through routine application of a computer model, that extreme pressure transients, created at the time, of several repeated pipe failure incidents on the same pipeline would exceed normal pipe working stresses. This arose in the circumstance where an air chamber had been taken out of service and no steps were taken for surge suppression by the operators. The computer analysis identified and simulated the effect of cavitation. The pipeline profile contained an intermediate high point, but no automatic air venting was incorporated. In circumstances where air (gas) pocket formations are possible (a highly likely situation in sewerage systems) and air venting is ineffective, it has been demonstrated here that peak pressures can be considerably enhanced over those arising from cavitation if the pocket volume is of some critical dimension at the time that the serious transient is generated.

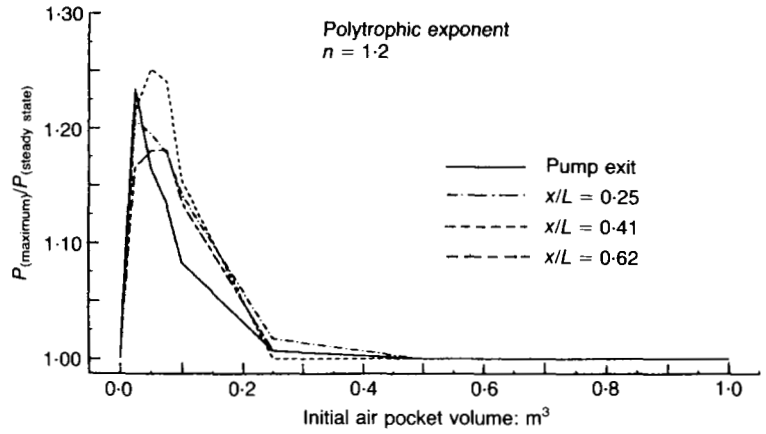

Fig. 11. Variation of ultimate maximum pressure duty, at sections along pipeline 'b', with increase in air pocket size (at x/L = 0·41), for delayed pump trip-out as detailed in Figure 10

44. It is the authors' view that such imponderables as possible air accumulation and, perhaps equally, air entrainment, which can have a serious effect on peak pressures, should be appraised and incorporated in analysis as a matter of routine where risk of surge exists. Those charged with assessment of pipeline protection should ensure that all feasible operational scenarios likely to give rise to severe transients are fully investigated and reported at the design stage. Of special relevance in this regard is the situation where surge suppression devices may be temporarily taken out of service for emergency repair or replacement while the station must remain in service.

Appendix 1

45. As the pump slows down after power failure, its head/discharge and torque/discharge characteristics change. It is customary to assume that, as the pump speed changes, the pump characteristics at any speed can be found using the similarity relationships for homologous pumps, as follows (Watters, 1979[20])

$$\frac{Q}{ND^3} = \text{constant}$$

$$\frac{HP}{N^2D^2} = \text{constant} \qquad (9)$$

$$\frac{T}{\rho N^2 D^5} = \text{constant}$$

where Q, HP, T and N are discharge, head increase (lift), torque and rotational speed respectively; D is pump dimension (generally the impeller diameter). For a particular unit, the homologous equations may be represented by

$$Q_2 = Q_1(N_2/N_1)$$
$$HP_2 = HP_1(N_2/N_1)^2 \qquad (10)$$
$$T_2 = T_1(N_2/N_1)^2$$

The subscripts refer to two homologous operating situations. For various speeds, the pump characteristics are calculated from the original curve at N_0.

46. The change in speed of pump rotation may be found by using the basic equation for torque as follows

$$T = -I(\mathrm{d}\omega/\mathrm{d}t) \qquad (11)$$

where I is the moment of inertia of rotating parts, including the liquid within the impeller; and $\mathrm{d}\omega/\mathrm{d}t$ is the angular acceleration. In a finite small time interval Δt, the torque is represented as the average of T_1, the known torque at beginning of Δt, and T_P, the unknown torque at the end of Δt. Integrating equation (11) and replacing angular velocity ω by rotation speed N yields

$$N_P = N_1 - \frac{15\Delta t}{\pi I}(T_P + T_1) \qquad (12)$$

This is the computational formula of rotational speed after power failure. Since there are two unknown values in equation (12), the new speed N_P cannot be determined. According to the homologous relationship, equation (10), however, $T_P = T_0(N_P/N_0)^2$, and eliminating T_P in equation (12) yields a quadratic equation as

$$N_P^2 + \frac{\pi I N_0^2}{15\Delta t T_0}N_P - \left(\frac{\pi I N_0^2}{15\Delta t T_0}N_1 - \frac{N_0^2}{T_0}T_1\right) = 0 \qquad (13)$$

in which subscript 0 denotes the steady-state condition; and subscript 1 designates the condition at beginning of Δt. The new rotational speed can now be determined explicitly using the known values of torque and speed. It is then possible to proceed with the calculation for the heads and discharges under transient conditions. The factors of the pump characteristic curve under new speed—β_1, β_2 and β_3—may be found by using a regression method.

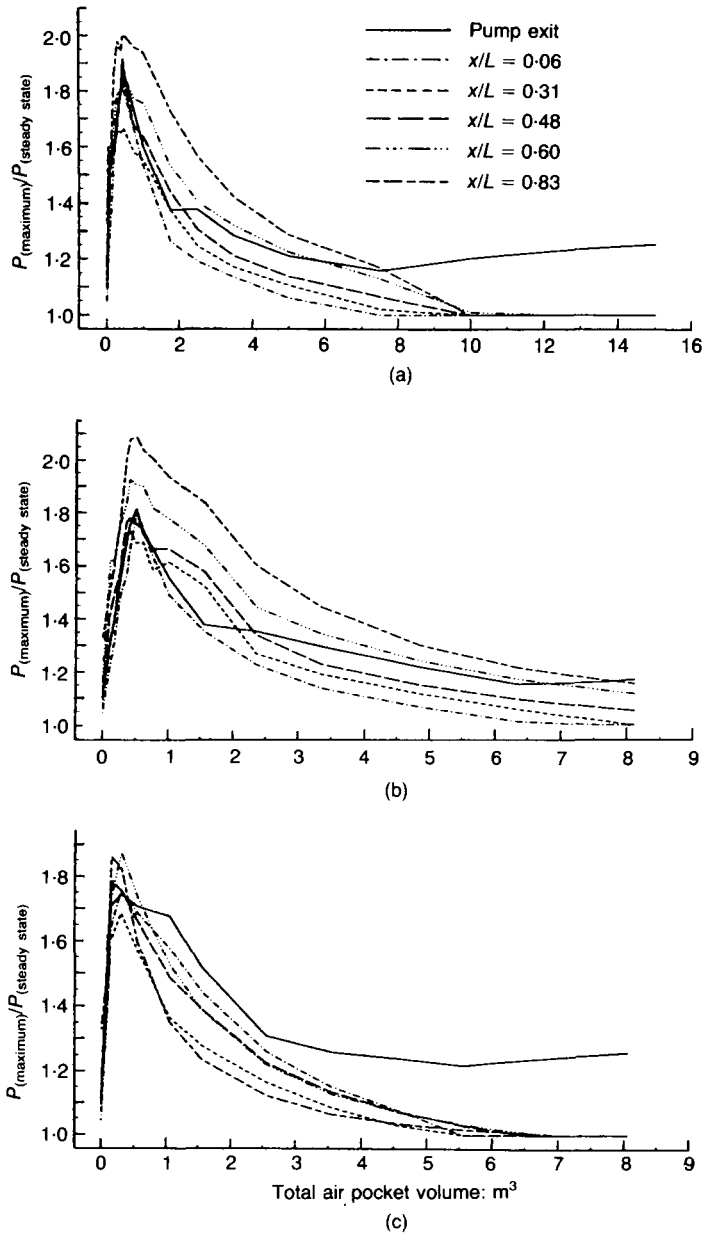

Fig. 12. Variation in ultimate maximum pressure duty at different sections along pipeline 'c' (Fig. 3) with air pockets at five high points and volume distributed: (a) equally; (b) linearly increasing downstream; (c) linearly decreasing downstream (Conditions single pump with check valve, initial steady flow 153·3 l/s; pump condition is same as Fig. 4; sump level 6·21 m; pipeline of pvc; station head loss coefficient ζ, 10·5)

References

1. Fox J. A. *Hydraulic analysis of unsteady flow in pipe networks*. MacMillan Press, London, 1977.
2. Twort A. C. *et al. Water supply*. Edward Arnold, London, 1994.
3. Wylie E. B. and Streeter V. L. *Fluid transients*. McGraw-Hill, New York, 1978.
4. Ewing D. J. F. Allowing for free air in water-hammer analysis. *Proc. 3rd Int. Conf. on Pressure Surges*. British Hydromechanics Research Association, Canterbury, 1980, 127–146.
5. Lee T. S. Numerical modelling and computation of fluid pressure transients with air entrainment in pumping installations. *Proc. Int. J. for Numerical methods in Fluids*, 1993, **19**, 89–103.
6. Whiteman K. J. and Pearsall I. S. *Reflux valve and surge tests at Kingston pumping station*. BHRA/National Engineering Laboratory, Glasgow, Joint Report 1, 1959.
7. Whiteman K. J. and Pearsall I. S. Reflux valve and surge tests at a station. *Fluid handling*, 1962, **XIII**, 248–250 and 282–286.
8. Dawson P. A. and Fox J. A. Surge analysis and suppression techniques for a water supply scheme—a case study. *Trans. Inst. meas. Control*, 1985, **5**, No. 4, 134–142.
9. Jönsson L. Maximum transient pressures in a conduit with check valve and air entrainment. *Proc. Int. Conf. on the Hydraulics of Pumping Stations*. British Hydromechanics Research Association, Manchester, 1985, 55–76.

10. THORLEY A. R. D. *Fluid transients in pipeline systems*. D. & L. George, 1991.
11. MARTIN C. S. Entrapped air in pipelines. *Proc. 2nd Int. Conf. on Pressure Surges*. British Hydromechanics Research Association, London 1976, F2-15–F2–28.
12. SAFWAT H. H., ARASTU A. H. and HUSAINI S. M. Generalized applications of the method of characteristics for the analysis of hydraulic transients involving empty sections. *Proc. 5th Int. Conf. on Pressure Surges*. British Hydromechanics Research Association, Hannover, 1986, 157–167.
13. LARSEN T. and BURROWS R. Measurements and computations of transients in pumped sewer plastic mains. *Proc. BHR Group/IAHR Int. Conf. on Pipeline Systems*, Manchester, 1992, 117–123.
14. JÖNSSON L. (BLAIN W. R. and KATSIFARAKIS K. L. (eds)). Leak detection in pipelines using hydraulic transients. *Hydraulic engineering software V, Vol. 1: Water resources and distribution*. Computational Mechanics publications, 1994, 344–352.
15. QIU D. Q. *Transient analysis and the effect of air pockets in a pipeline*. Department of Civil Engineering, University of Liverpool, 1995, MPhil thesis.
16. LARSEN T. *Waterhammer at pump shutdown (WHPS)*. Torben Larsen Hydraulics Aps, Aalborg, 1992, Programme User Guide, version 2.13.
17. WYLIE E. B. Fundamental equations of waterhammer. *J. Hydraul. Engng, Am. Soc. Civ. Engrs*, 1984, **110**, No. 4, 539–542.
18. WYLIE E. B. Closure to discussions on 'Fundamental equations of waterhammer'. *J. Hydraul. Engng, Am. Soc. Civ. Engrs*, 1985, **111**, No. 8, 1197–1200.
19. CHAUDHRY M. H. Seminar C: Limitations of hydraulic–transient computations. *Proc. 21st IAHR Congr.*, Melbourne, 1985, **6**, 132–137.
20. WATTERS G. Z. *Modern analysis and control of unsteady flow in pipelines*. Ann Arbor Science Publishers, Ann Arbor, 1979.
21. LARSEN T. *Description of the demo program: WHPSDEMO*. Torben Larsen Hydraulics Aps, Aalborg, 1992.